POLITECNICO DI TORINO
Repository ISTITUZIONALE

A Statistical Assessment of Opto-Electronic Links

*Original*
A Statistical Assessment of Opto-Electronic Links / Manfredi, P., Stievano, I.S., Perrone, G., Bardella, P., Canavero, F.. - STAMPA. - (2012), pp. 61-64. (21st IEEE International Conference on Electrical Performance of Electronic Packaging and Systems (EPEPS) Tempe, AZ, USA Oct. 21 -24) [10.1109/EPEPS.2012.6457843].

*Availability:*
This version is available at: 11583/2505648 since:

*Publisher:*
IEEE

*Published*
DOI:10.1109/EPEPS.2012.6457843

*Terms of use:*

This article is made available under terms and conditions as specified in the corresponding bibliographic description in the repository

*Publisher copyright*

(Article begins on next page)

09 November 2026

# A Statistical Assessment of Opto-Electronic Links

Paolo Manfredi, Igor S. Stievano, Guido Perrone, Paolo Bardella, Flavio G. Canavero

DET – Department of Electronics and Telecommunications, Politecnico di Torino
10129 Torino, Italy {igor.stievano@polito.it}

***Abstract*—This paper addresses the stochastic simulation of high-speed optical interconnects. It provides an effective solution for the inclusion of the effects of process variation or possible unknown device characteristics on the system response. The proposed approach is based on the stochastic collocation method and Lagrange interpolation. The results obtained on the transient analysis of a realistic on-board optical link with uncertain parameters conclude the paper.**

***Index Terms*—Circuit modeling, circuit simulation, optical interconnects, stochastic analysis, stochastic collocation, tolerance analysis, uncertainty.**

## I. Introduction

Recent progress in developing high density and low cost optical interconnects and devices for board and backplane applications demands for the availability of fully integrated simulation environments [1], [2]. Numerical simulation has been consolidated as a tool for virtual prototyping, thus allowing the assessment of the performance of alternative design scenarios in the very early design phase. In this framework, the availability of efficient methods accounting for possible parameter variabilities due to, e.g., the manufacturing process, is highly desirable for supporting designers in setting the right design margins.

The typical resource allowing to collect quantitative information on the statistical behavior of system responses is based on the application of the blind and brute-force Monte Carlo (MC) method [3]. Such method, however, is computationally expensive, thus making its application to the analysis of complex realistic structures prohibitive.

The high computational cost that characterizes MC simulations is due to the fact that it does not exploit possible regularities of the random parameters. When the dependence on the random parameters is smooth and can be expressed in terms of polynomial functions with reasonable accuracy, polynomial chaos (PC) framework provides efficient tools to overcome the previous limitation and handle the stochasticity directly into the governing equation [4], [5]. These methodologies allow to represent the stochastic solution of a dynamical system in terms of orthogonal polynomials of random variables. Examples in the area of interest are the extensions of the classical circuit analysis tools – possibly in a SPICE environment – to the prediction of the stochastic behavior of lumped circuits with uncertain parameters [6], or distributed interconnects described by transmission-line equations [7], or a combination of both [8].

However, when the random variables of interest appear in a nonlinear form inside the governing equations, the class of stochastic collocation methods (SCMs) turns out to be a more effective alternative [4], [9]. Generally speaking, the SCM is based on a clever sampling of the random space and on a suitable interpolation of the stochastic response of a dynamical system. In this paper, the SCM technique, combined with Lagrange interpolation [4], is used for the transient simulation of a realistic printed circuit board (PCB) structure with an embedded optical fiber interconnect with uncertain parameters. This structure, that is governed by nonlinear dynamical equations, clearly benefits from the application of the advocated method.

## II. Application test case: on-board optical link

The scheme of Fig. 1 represents a typical opto-electronic link consisting of the cascade connections of a number of basic building blocks. The transmitting laser diode $L$, the optical junctions $J1$ and $J2$, the optical interconnect $F$ and the receiving photodiode $D$ are highlighted in this structure.

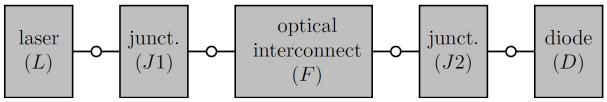


Fig. 1. Block diagram of a PCB opto-electronic link.

The simulation of the link of Fig. 1 is carried out by using the simplified governing equations of the different blocks. In particular, the semiconductor laser is modeled using its physical-based rate-equations in the mean field approximation [10]

$$\begin{cases} \dfrac{dN(t)}{dt} = \dfrac{i_d(t)}{qV_l} - \dfrac{N(t)}{\tau_n} - \dfrac{G_0(N(t)-N_0)S(t)}{1+\varepsilon S(t)} \\ \dfrac{dS(t)}{dt} = \dfrac{\Gamma G_0(N(t)-N_0)S(t)}{1+\varepsilon S(t)} - \dfrac{S(t)}{\tau_p} + \Gamma\beta\dfrac{N(t)}{\tau_n}. \end{cases} \quad (1)$$

where, for the sake of simplicity, a single operation mode of the laser is considered. The state variables $N$ and $S$ are the semiconductor carrier and photon densities, respectively, while $i_d$ is the electrical injected current. It contains the information that must be sent through the optical link, and is generated by the electronics controlling the optical module. In other words, $i_d$ represents the source term for the above equations.

Also, $q$ is the electron charge, $V_l$ is the active region volume, $G_0$ is the linear gain coefficient, $\varepsilon$ is the gain compression factor. Moreover, $\tau_n$ and $\tau_p$ are the carrier and photon lifetimes, respectively, while $N_0$ is the transparency carrier density, $\Gamma$ is

the transversal mode confinement factor and $\beta$ is the fraction of spontaneous emission coupled into the laser mode.

According to [10], the output optical transmitted power $p(t)$, sent along the fiber, is given by

$$p(t) = \frac{S(t)V_l\eta_0 h\nu}{2\Gamma\tau_p}, \tag{2}$$

where $\eta_0$ is the differential quantum efficiency, $h$ is the Planck's constant and $\nu$ the unmodulated optical frequency.

The junctions and the optical fiber are assumed to be described by idealized blocks defined by attenuation constants only. This assumption is justified by the specific application at hand, that involves relatively short on-board optical interconnects.

The last block of the chain, i.e., the photodiode detector, is described by a simple static model, whose function is to generate an electrical current proportional to the received optical power. This current extracts the signal injected in the optical link by $i_d$ defined above, and represents the source of the electronic stage performing the processing of information. Therefore, the current $i(t)$ through the photodiode is expressed by

$$i(t) = \alpha_1\alpha_f\alpha_2\alpha_d p(t), \tag{3}$$

where $\alpha_{1,2}$, $\alpha_f$ and $\alpha_d$ are the attenuation factors introduced by the corresponding blocks $J1$, $J2$, $F$ and $D$ in Fig. 1, respectively.

Clearly, equations (1)–(3) represent a set of nonlinear dynamical equations, whose parameters may vary due to different possible choices of the commercial components considered in a specific design, or even to the process variability affecting the behavior of different samples of the same component.

In the example test case considered in this study, the optical interconnect is 20 cm long and has an attenuation of 0.1 dB/cm ($\alpha_f = 2$ dB). Also, the laser has a wavelength of 850 nm and is defined by the set of parameters in [10]. The nominal attenuation factors of the junctions and of the photodiode are $\alpha_1 = \alpha_2 = 0.13$ and $\alpha_d = 0.9$, respectively. For a given set of model parameters, the simulation of the opto-electronic link of Fig. 1 requires a numerical solution of (1)–(3), which is carried out by means of the integration routines available in the Matlab® environment.

It is worth noting that a more accurate description of the link can be adopted (e.g., when one wishes to account for the multimode propagation in the optical medium or the effects of the reflected wave). An extended formulation would not limit the applicability of the method illustrated in the following Sections.

## III. Impact of process variation

A detailed discussion of the technological aspects impacting the electrical performance of an optical interconnect like the one in Fig. 1 is out of the scope of this paper. Among the different sources of variations, in this study we select and focus on three parameters (namely, $G_0$, $\alpha_1$ and $\alpha_2$) that have been demonstrated to be major sources of uncertainty with a large impact on the interconnect performance. The gain coefficient $G_0$ is included in the nonlinear dynamical equation of the laser and varies within a sufficiently large range for different alternative laser devices. The remaining two parameters, $\alpha_1$ and $\alpha_2$, account for the possible uncertainty coming from the misalignment of the coupling between the optical waveguide and the laser diode/detector. Of course, the values of the latter parameters depend on the specific implementation design. Readers are referred to [11] for three possible alternative designs and information on their respective variability range. In the above paper, the transition between the laser device mounted on the board and the optical interconnect emedded in the PCB is achieved via $(i)$ an optical subssembly placed in a hole drilled or etched to the PCB, $(ii)$ micro-lens and $(iii)$ micro-sized-ball lens.

The above parameters, that are assumed to vary within a bounded interval, can be conveniently rewritten as follows:

$$\begin{cases} \alpha_1 &= \bar{\alpha}_1 + (\Delta\alpha_1/2)\xi \\ \alpha_2 &= \bar{\alpha}_2 + (\Delta\alpha_2/2)\eta \\ G_0 &= \bar{G}_0 + (\Delta G_0/2)\gamma, \end{cases} \tag{4}$$

where $\xi$, $\eta$ and $\gamma$ are independent uniform random variables with probability density function 0.5 over the domain [-1,1].

It should be noted that the three normalized distributions are assumed to be statistically independent even if some correlation among the parameters exists (e.g., see [12]). However, this does not represent a limitation, as correlated random variables can be represented in terms of independent ones [5].

The variability of the model parameters unavoidably makes the responses of the opto-electronic link stochastic variables as well. As an example, the output optical transmitted power $p(t, \boldsymbol{\xi})$ will depend on the vector $\boldsymbol{\xi} = [\xi, \eta, \gamma]^T$, that collects the three uniform random variables in (4). The same holds for the other variables of interest, like the current detected by the photodiode $i(t, \boldsymbol{\xi})$.

## IV. The stochastic collocation method

This section provides an overview of the proposed SCM technique with a brief discussion of the three main features of the Lagrange interpolation, i.e., the interpolating polynomials, the clever choice of the collocation points and the extension to account for multiple random variables.

### A. Lagrange interpolation

The basic idea of the SCM and Lagrange interpolation is to sample the stochastic system response at (few) clever points and to reconstruct the overall response in the whole random space by interpolation. For a time-domain response $y(t, \xi)$ depending on a single random variable $\xi$, the interpolation is

$$y(t, \xi) \approx \sum_{i=0}^{P} y(t, \xi_i)\Phi_i(\xi), \tag{5}$$

where $\{\Phi_i\}$ are the Lagrange polynomials associated to the collocation points $\xi_i$. They are built as

$$\Phi_i(\xi) = \prod_{\substack{0\le j\le P \\ j\neq i}} \frac{\xi - \xi_j}{\xi_i - \xi_j}, \tag{6}$$

and the following property holds:

$$\Phi_i(\xi_j) = \delta_{ij} \tag{7}$$

where $\delta_{ij}$ is the Kronecker's delta.

Clearly, (5) turns out to be an analytical function where a limited set of responses $y(t, \xi_i)$, evaluated for specific samples $\xi_i$ of the random variable $\xi$, are used to reconstruct the continuous behavior by means of Lagrange polynomials. Such an analytical expression can be used as a computationally-cheap model for a fast sampling of the random response and extraction of statistical information. Of course, when $y(t, \xi)$ can be exactly represented as a $P$th-order polynomial, (5) turns out to be exact.

### B. Choice of the collocation points

One key issue of the solution consists in finding a good set of collocation points where to evaluate the random response. Although different choices are available, the analogy with Gaussian quadratures suggests to use the roots of the polynomials which are orthogonal to the distribution of the random variable $\xi$. For standard distributions, such as Gaussian or uniform, these polynomials are well-known and correspond to Hermite and Legendre polynomials, respectively. Hence, in the case of uniform variability, for a given value of $P$ in (5), the points $\xi_i$ are given by the roots of the $(P+1)$th-order Legendre polynomial. For instance, if $P = 3$, we have four evaluation points at $\xi = \pm\sqrt{(3 + 2\sqrt{6/5})/7}$ and $\xi = \pm\sqrt{(3 - 2\sqrt{6/5})/7}$.

### C. Extension to multiple random variables

A straightforward generalization to the case of multiple random variables is to use a multivariate interpolation where the collocation points are represented by a tensor product grid obtained from the one-dimensional case. In turn, the multivariate Lagrange polynomials are built as products of univariate polynomials. For example, given two random variables $\xi$ and $\eta$, the two-dimensional collocation grid is represented by all the possible points $\boldsymbol{\xi}_i = (\xi_m, \eta_n)$ with $m \leq P_1$ and $n \leq P_2$. It should be noted that a square grid (i.e., $P_1 = P_2 = P$) is usually employed, but this is not mandatory. Moreover, the bivariate Lagrange polynomials are obtained as

$$\Phi_i(\boldsymbol{\xi}) = \Phi_i(\xi, \eta) = \Phi_m(\xi)\Phi_n(\eta), \quad \begin{matrix} m \leq P_1 \\ n \leq P_2. \end{matrix} \tag{8}$$

The total number of response samples to be computed is thus

$$Q = \prod_{k=1}^{n} (P_k + 1), \tag{9}$$

where $n$ is the number of random variables. For large values of $P_k$ and/or $n$, sparse grids allow to contain the excessive increment in the number of evaluations [4].

## V. Numerical results

In this section, the stochastic simulation of the optical link of Fig. 1 is performed by considering the random variations expressed in (4). The nominal values are $\bar{G}_0 = 1.5 \times 10^{-12}$ m$^3$/s and $\bar{\alpha}_1 = \bar{\alpha}_2 = 0.13$, while the intervals of variation are assumed to be $\Delta G_0 = 0.6 \cdot \bar{G}_0$ and $\Delta\alpha_1 = \Delta\alpha_2 = 0.03$ (see [11] for the order of magnitude of the variability of $\alpha_1$ and $\alpha_2$). The laser is driven by a 1 GHz non-return-to-zero pseudo-random bit stream and the propagation of the signal through the link is carried out by solving equations (1)–(3).

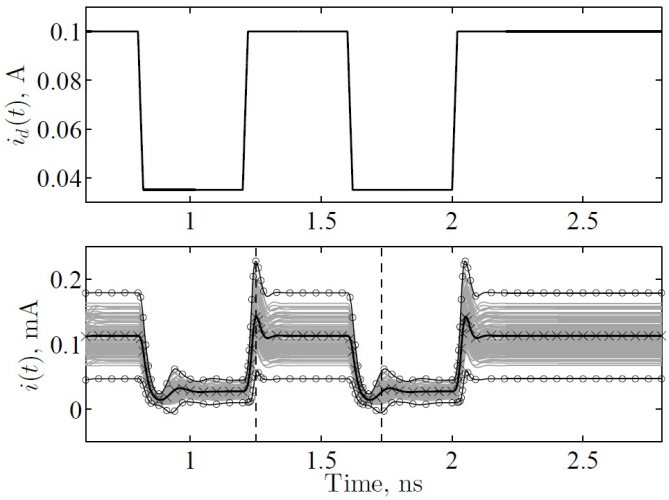


Fig. 2. Current injected into the laser (top panel) and photodiode output current (bottom panel). Gray lines: a sample of responses, limited to 100 curves for graph readability; solid black lines: mean value and $\pm 3\sigma$ limits computed with MC; crosses and circles: mean value and $\pm 3\sigma$ limits obtained by means of the SCM.

Fig. 2 shows the input injected current $i_d(t)$ as well as the current $i(t)$ detected by the photodiode. Clearly, the latter is a random variable due to the uncertainties introduced by the laser and the optical link. As such, it exhibits a spread of different possible values. The mean value and the $\pm 3\sigma$ limits of this spread are estimated by means of both 10000 MC simulations and the SCM, showing excellent agreement. In the latter case, a three-dimensional grid with a total of $Q = 16$ points has been used.

Nonethless, designers may be interested in more quantitative statistical information, like probability density functions (PDFs). These can be obtained from the SCM as well. The problem amounts to computing the PDF of an analytical function, like (5), that is applied to the original random variables, and this can be fast and straightforwardly achieved via numerical techniques. Fig. 3 shows the PDFs of $i(t)$ computed at two different time points – indicated by the vertical dashed lines in Fig. 2 – again with both MC and the SCM. The strength and accuracy of the SCM are confirmed by its capability of correctly reproducing the distribution shapes obtained with the standard MC technique.

Finally, Tab. I summarizes the key figures about the efficiency of the advocated method, showing that the SCM is

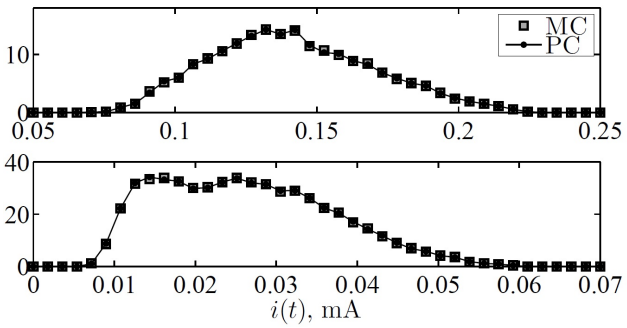


Fig. 3. Probability density function of the output photodiode current, computed at two different time points.

TABLE I
CPU TIME REQUIRED BY MC AND SCM SIMULATIONS.

| Method | Number of samples | Total simulation time | Speed-up |
|---|---|---|---|
| MC | 10 000 | 3 h 40 min | – |
| SCM | 16 | 21 s | $\sim 625\times$ |

over 600 times faster than the traditional MC approach in the simulation of the link of Fig. 1 in presence of three sources of random variations.

## VI. CONCLUSIONS

The simulation of high-speed optical links with the inclusion of the effects of process variation or possible unknown device parameters has been addressed in this contribution. The proposed technique belongs to the class of stochastic collocation methods and Lagrange interpolation and provides an effective solution to the stochastic simulation of nonlinear dynamical systems.

It provides a clever exploration and subsequent interpolation of the random space of the system solutions, yet allowing the prediction of the model behavior from a limited number of system simulations.

The advocated method, while providing accurate results, turns out to be more efficient than the classical Monte Carlo technique in determining the effects of parameters variability on the system response. The feasibility and strength of the proposed approach are demonstrated for a realistic on-board optical link and time-domain analysis.

## REFERENCES

[1] R. Nagarajan et Al., "Large-scale photonic integrated circuits", *IEEE Journal of Selected Topics in Quantum Electronics,* vol. 11, no. 1, pp. 50–65, Jan./Feb. 2005.

[2] P. Gunupudi, T. Smy, J. Klein and J. Jakubczyk, "Self-consistent simulation of opto-electronic circuits using a modified nodal analysis formulation", *IEEE Transactions on Advanced Packaging,* vol. 33, no. 4, pp. 979–993, Nov. 2010.

[3] Q. Zhang, J. J. Liou, J. McMacken, J. Thomson and P. Layman, "Development of robust interconnect model based on design of experiments and multiobjective optimization," *IEEE Transactions on Electron Devices,* vol. 48, no. 9, pp. 1885–1891, Sep. 2001.

[4] D. Xiu, "Fast numerical methods for stochastic computations: a review", *Communications in Computational Physics,* vol. 5, no. 2–4, pp. 242–272, Feb. 2009.

[5] R. G. Ghanen and P. D. Spanos, *Stochastic Finite Elements. A Spectral Approach.* New York: Springer-Verlag, 1991.

[6] K. Strunz and Q. Su, "Stochastic formulation of SPICE-type electronic circuit simulation using polynomial chaos," *ACM Trans. Model. Comput. Simul.,* vol. 18, no. 4, pp. 15:1–15:23, Sep. 2008.

[7] I. S. Stievano, P. Manfredi and F. G. Canavero, "Parameters variability effects on multiconductor interconnects via Hermite polynomial chaos," *IEEE Trans. Compon., Packag. Manuf. Technol.,* vol. 1, no. 8, pp. 1234-1239, Aug. 2011.

[8] P. Manfredi, I. S. Stievano and F. G. Canavero, "Alternative SPICE implementation of circuit uncertainties based on orthogonal polynomials," in *Proc. IEEE 20th Conf. Electr. Perform. Electron. Pack. Sys.,* Oct. 2011, pp. 41–44.

[9] A. Rong and A. C. Cangellaris, "Interconnect transient simulation in the presence of layout and routing uncertainty", in *Proc. IEEE 20th Conf. Electr. Perform. Electron. Pack. Sys.*, Oct. 2011, pp. 41–44.

[10] J. C. Cartledge and R. C. Srinivasan, "Extraction of DFB laser rate equation parameters for system simulation purposes", *IEEE Journal of Lightwave Technology,* vol. 15, no. 5, May 1997.

[11] M. Karppinen et Al., "Optical interconnect on printed wiring board," in *Proc. of SPIE*, vol. 5358, 2004, pp. 135–145.

[12] L. A. Coldren, S. W. Corzine and M. L. Mashanovitch, *Diode Lasers and Photonic Integrated Circuits.* New York: Wiley, Mar. 2012, 2$^{\text{nd}}$ edn.